



HAL
open science

First infrared investigations of OCS–H₂O, OCS–(H₂O)₂, and (OCS)₂–H₂O complexes isolated in solid neon: Highlighting the presence of two isomers for OCS–H₂O

P. Soulard, B. Madebène, B. Tremblay

► **To cite this version:**

P. Soulard, B. Madebène, B. Tremblay. First infrared investigations of OCS–H₂O, OCS–(H₂O)₂, and (OCS)₂–H₂O complexes isolated in solid neon: Highlighting the presence of two isomers for OCS–H₂O. *The Journal of Chemical Physics*, 2017, 146 (23), pp.234303. 10.1063/1.4986403. hal-01587670

HAL Id: hal-01587670

<https://hal.sorbonne-universite.fr/hal-01587670v1>

Submitted on 14 Sep 2017

HAL is a multi-disciplinary open access archive for the deposit and dissemination of scientific research documents, whether they are published or not. The documents may come from teaching and research institutions in France or abroad, or from public or private research centers.

L'archive ouverte pluridisciplinaire **HAL**, est destinée au dépôt et à la diffusion de documents scientifiques de niveau recherche, publiés ou non, émanant des établissements d'enseignement et de recherche français ou étrangers, des laboratoires publics ou privés.

First infrared investigations of OCS–H₂O, OCS–(H₂O)₂, and (OCS)₂–H₂O complexes isolated in solid neon: Highlighting the presence of two isomers for OCS–H₂O

P. Soulard, B. Madebène, and B. Tremblay

Citation: *The Journal of Chemical Physics* **146**, 234303 (2017); doi: 10.1063/1.4986403

View online: <http://dx.doi.org/10.1063/1.4986403>

View Table of Contents: <http://aip.scitation.org/toc/jcp/146/23>

Published by the [American Institute of Physics](#)

Articles you may be interested in

[Structure and binding energy of the H₂S dimer at the CCSD\(T\) complete basis set limit](#)

The Journal of Chemical Physics **146**, 234301 (2017); 10.1063/1.4985094

[Water-anion hydrogen bonding dynamics: Ultrafast IR experiments and simulations](#)

The Journal of Chemical Physics **146**, 234501 (2017); 10.1063/1.4984766

[A quantum-mechanical perspective on linear response theory within polarizable embedding](#)

The Journal of Chemical Physics **146**, 234101 (2017); 10.1063/1.4985565

[High resolution jet-cooled infrared absorption spectra of \(HCOOH\)₂, \(HCOOD\)₂, and HCOOH–HCOOD complexes in 7.2 μm region](#)

The Journal of Chemical Physics **146**, 244306 (2017); 10.1063/1.4989863

[Assessment of two hybrid van der Waals density functionals for covalent and non-covalent binding of molecules](#)

The Journal of Chemical Physics **146**, 234106 (2017); 10.1063/1.4986522

[Dynamics, magnetic properties, and electron binding energies of H₂O₂ in water](#)

The Journal of Chemical Physics **146**, 234502 (2017); 10.1063/1.4985667



Scilight

Sharp, quick summaries **illuminating**
the latest physics research

Sign up for **FREE!**

AIP
Publishing

First infrared investigations of OCS–H₂O, OCS–(H₂O)₂, and (OCS)₂–H₂O complexes isolated in solid neon: Highlighting the presence of two isomers for OCS–H₂O

P. Soulard,^{a)} B. Madebène, and B. Tremblay

Sorbonne Universités, UPMC Univ Paris 06, CNRS, UMR 8233, MONARIS, Case Courrier 49, Université Pierre et Marie Curie, 4 Place Jussieu, F-75005 Paris, France

(Received 9 March 2017; accepted 5 June 2017; published online 19 June 2017)

For the first time, complexes involving carbonyl sulfide (OCS) and water molecules are studied by FTIR in solid neon. Many new absorption bands close to the known fundamental modes for the monomers give evidence for at least three (OCS)_n–(H₂O)_m complexes, noted n:m. With the help of theoretical calculations, two isomers of the 1:1 complex are clearly identified. Concentration effects combined with a detailed vibrational analysis allow for the identification of transitions for the 1:1, 1:2, and 2:1 complexes. Anharmonic coupling constants have been derived from the observations of overtones and combinations. *Published by AIP Publishing.* [<http://dx.doi.org/10.1063/1.4986403>]

I. INTRODUCTION

The van der Waals complexes formed by small molecules and water have attracted considerable theoretical and experimental interest due to their importance in atmospheric and environmental chemistry.¹ Several linear triatomic molecules (CO₂, OCS, N₂O, SeCO) complexed with water have been studied.^{2–11} For the OCS–H₂O complex, few theoretical works^{3–10} have been published, and only one experimental study in the gas phase exists in the microwave domain.¹⁰ The most stable calculated structure has a C_{2v} symmetry, which is consistent with the experimental evidences,¹⁰ the sulfur atom being bonded to the water oxygen; the calculated binding energy is of 5.5 kJ/mol.^{4,8,9} Besides, other structures are predicted^{3,4,6} with slightly weaker binding energies. For the 1:2 complex, there is no experimental data, and this species has been the subject of only two theoretical studies.^{4,9} There is no data for the 2:1 complex, but the OCS dimer (2:0) has been well studied in theoretical works^{12–14} and the infrared data were obtained by the McKellar group with a tunable diode laser in the region of the C–O fundamental stretching mode.^{15–17} Since no infrared study has been published, we sought to study the (OCS)_n–(H₂O)_m complexes in a neon matrix to obtain new vibrational data from the far to the near infrared (50–7000 cm^{−1}). Recently, we have shown that it is possible to obtain some new vibrational data in solid neon for the hydrated (CO₂)_n–(H₂O)_m complexes.² We also performed *ab initio* calculations with the aim of obtaining homogeneous results (same method and basis set) to be compared with the experimental data for the most stable isomers of the 1:1, 2:0, 0:2, 1:2, and 2:1 complexes.

After a brief description of the experimental conditions, experimental spectra will be presented, an assignment of the different bands will be proposed and a comparison with our theoretical results will be discussed.

II. EXPERIMENTAL AND THEORETICAL DETAILS

A. Experimental apparatus

Samples were prepared by co-condensing OCS–Ne and H₂O–Ne mixtures at a rate of 2–15 mmol/h onto one of the six highly polished, rhodium-plated copper mirrors maintained at 3 K using a closed-cycle helium cryostat (Cryomech PT-405).

All the spectra have been recorded at 3 K. The temperature was measured using silicon diodes and the thermal annealing in the 8–12 K range was regulated by a Neocera LTC-II temperature controller. The Ne/OCS mole ratio varied between 30 and 30 000, and the neon/water mole ratio between 1000 and 20 000 but variable desorption of water from the stainless steel vacuum line precluded accurate concentration measurements, and the uncertainty of the H₂O final concentration is around 30%. Absorption spectra were recorded between 50 and 7000 cm^{−1} on the same sample using a Bruker 120 FTIR spectrometer equipped with suitable combinations of light sources (globar, W filament), beamsplitters (composite, KBr/Ge, Si/CaF₂), and detectors (liquid N₂-cooled InSb, liquid N₂-cooled HgCdTe photoconductor, liquid He-cooled Si–B bolometer). The resolution was fixed to 0.1 cm^{−1}. A natural water sample was degassed under vacuum before use. Ne (Air Liquide, 99.995% purity) and OCS (Aldrich, 99.9% purity) were used without purification.

B. Computational details

All calculations have been performed with the augmented correlation-consistent basis set aug-cc-pVTZ (AVTZ) of Dunning and co-workers.^{18,19} Second order Møller-Plesset calculations (MP2) were performed with the Gaussian09 package,²⁰ while explicitly correlated coupled cluster calculations [CCSD(T)-F12a] were performed with the Molpro2012 package.^{21,22}

(OCS)_n–(H₂O)_m (m = 0–2, n = 0–2) species structures were optimized with “verytight” convergence criteria, followed by harmonic frequencies calculation at MP2/AVTZ level of theory. These calculations lead to equilibrium

^{a)} Author to whom correspondence should be addressed: pascale.soulard@upmc.fr

geometries, equilibrium (D_e) and ground state (D_0) binding energies, harmonic vibrational frequencies, and infrared intensities.

Due to computational limitation, only monomers and the 1:1 complex have been fully investigated (geometry optimization and harmonic frequencies calculation) at CCSD(T)-F12a/AVTZ level of theory. For 2:0, 0:2, 1:2, and 2:1 complexes, single point CCSD(T)-F12a/AVTZ energy calculations have been performed at MP2/AVTZ optimized structures to compute equilibrium binding energies (D_e^*), and MP2/AVTZ zero point energy correction (ZPE) has been used to compute ground state binding energies (D_0^*).

III. SPECTRAL DATA AND ASSIGNMENTS

The infrared absorptions of the H_2O monomer, dimer, and trimer trapped in solid neon are well known for the fundamental modes, and for many overtones and combinations.^{23,24} Few studies^{25,26} have been done on the OCS monomer in matrix, and the only available experimental data on the OCS dimer^{15–17} and trimer^{27,28} were obtained by the McKellar group in a supersonic slit-jet expansion of a He/OCS gas mixture probed with a tunable diode laser in the region of the C–O fundamental stretching mode.

Our experiments were performed using different concentration ratios of the OCS/ H_2O /Ne gas mixture to identify the transitions of the $n:m$ complexes: low concentration, typically OCS/ H_2O /Ne = 0.02/0.5/1000 for the 1:1 complex and OCS/ H_2O /Ne = 1/0.2–1/1000 and 1–15/0.06/1000 for 1: m and n :1 complexes, respectively. Thermal annealing permits diffusion of the molecules in the sample and enhances the intensity of the bands of many $m:n$ complexes, and especially those of the 0:2, 2:0, 1:2, and 2:1 ones that will be studied in this work.

Figures 1–7 illustrate the IR spectra in different frequency ranges. Tables I–III summarize our measured vibrational frequencies of $(OCS)_n-(H_2O)_m$ complexes: Table I for the monomers and the 1:1 complex, Table II for the H_2O dimer and the 1:2 complex, and Table III for the OCS dimer and the 2:1 complex.

A. OCS spectral regions

Since there is no data on OCS isolated in solid neon, we first examine the spectrum of OCS/Ne deposition

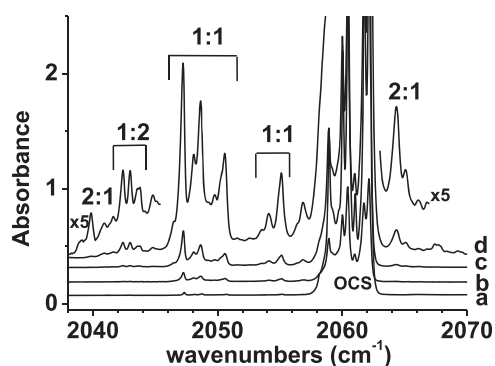


FIG. 1. Spectra in the OCS stretching ν_3 region at 3 K deposition, with different OCS/ H_2O /Ne concentration ratios. (a) 0.1/0/1000, (b) 0.03/1/1000, (c) 0.15/1/1000, (d) 1/1/1000.

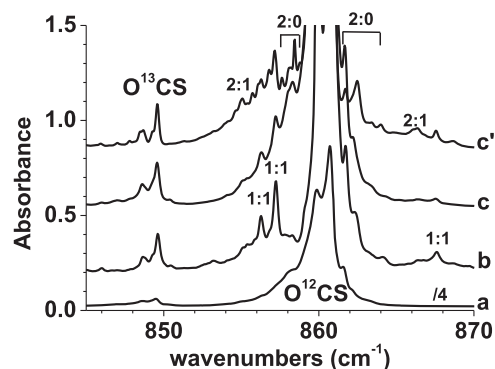


FIG. 2. Spectra in the OCS stretching ν_1 region at 3 K deposition, with different OCS/ H_2O /Ne concentration ratios. (a) 15/0/1000, (b) 5/1/1000, (c) 15/0.06/1000, (c') spectrum (c) followed by annealing at 12 K.

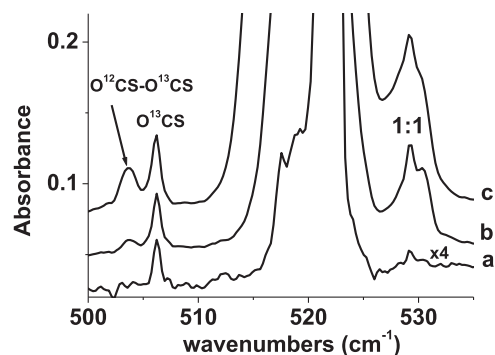


FIG. 3. Spectra in the OCS bending mode ν_2 region at 3 K deposition, with different OCS/ H_2O /Ne concentration ratios. (a) 3/0/1000, (b) 15/0.06/1000, (c) 30/0.06/1000. Each spectrum was normalized with respect to the OCS monomer intensity.

without water [Fig. 1(a)]. We observe three strong bands, due to different sites, with a main band located at 2062.2 cm^{-1} for the ν_3 ^{12}C –O stretching mode, same value as in gas phase.²⁹ In all this work, we will use the Hertzberg's convention for linear triatomic molecule: ν_3 and ν_1 for the C–O and C–S stretching modes, respectively, and ν_2 for the bending mode. Near the monomer's fundamentals we observe many bands for the OCS dimer, especially at higher concentration at 2067.6 ,

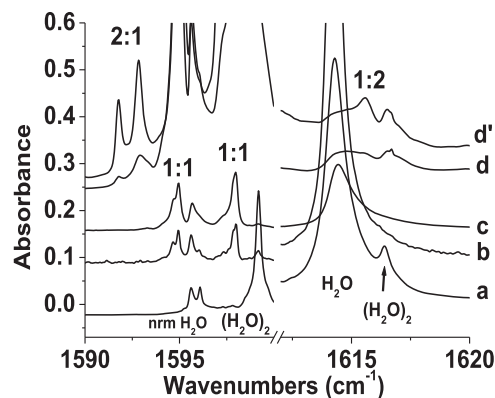


FIG. 4. Spectra in the H_2O bending mode ν_2 region at 3 K deposition, with different OCS/ H_2O /Ne concentration ratios. (a) 0/0.3/1000, (b) 0.3/0.06/1000, (c) 0.5/0.06/1000, (d) 15/0.06/1000, (d') spectrum (d) followed by annealing at 12 K. The spectra a, b, and c were normalized with respect to the ν_2 of nrm H_2O .

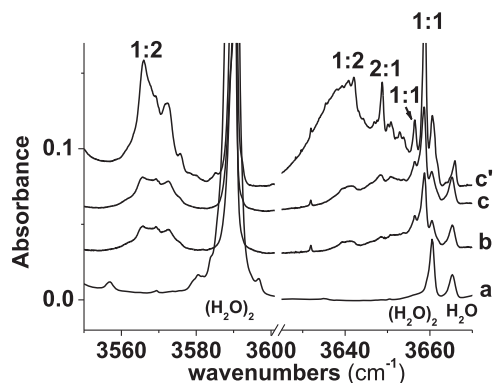


FIG. 5. Spectra in the 3550-3670 cm^{-1} region at 3 K deposition, with different OCS/ H_2O /Ne concentration ratios. (a) 0/0.3/1000, (b) 7.5/0.06/1000, (c) 15/0.06/1000, (c') spectrum (c) followed by annealing at 12 K. The spectra were normalized with respect to the ν_1 of nrm H_2O .

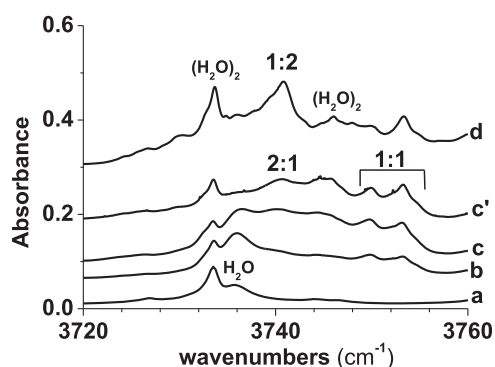


FIG. 6. Spectra in the 3720-3760 cm^{-1} region at 3 K deposition, with different OCS/ H_2O /Ne concentration ratios. (a) 0/0.3/1000, (b) 7.5/0.06/1000, (c) 15/0.06/1000, (c') spectrum (c) followed by annealing at 8 K, (d) 5/1/1000.

858.3, and 521.3 cm^{-1} (Table III and Figs. 1–3). The annealing effects confirm these attributions. With addition of water, in Figs. 1(b)–1(d), two groups of bands appear with a similar multiple sites pattern. The first group, more red shifted, is composed of bands at 2047.3 (the most intense), 2048.7, and 2050.7 cm^{-1} , and the second with two bands at 2054.1 and 2055.1 cm^{-1} (the most intense). Note that we observe the band at 2047.3 cm^{-1} in the spectrum with only OCS/Ne deposition because of the presence of water traces due to wall degassing.

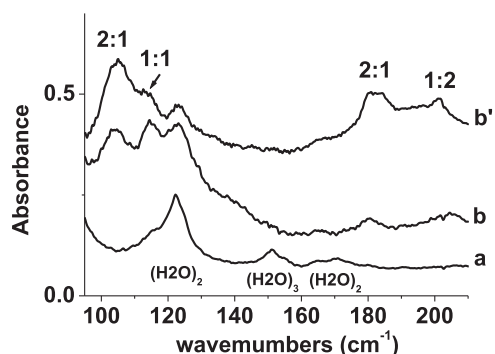


FIG. 7. Spectra in the 90-210 cm^{-1} region at 3 K deposition, with different OCS/ H_2O /Ne concentration ratios. (a) 0/0.3/1000, (b) 15/0.06/1000, (b') spectrum (b) followed by annealing at 12 K.

TABLE I. Observed frequencies (cm^{-1}) and assignments for OCS and H_2O monomers, and OCS- H_2O complex isolated in solid neon. Most intense bands are in bold.

n:m	Assignment	OCS	H_2O	ν_i^a
1:1				115
OCS	ν_2	521.7		
1:1	ν_2	529.3 , 530.6		
1:1	ν_1	857.2 , 867.6		
OCS	ν_1	860.9		
OCS	$2\nu_2$	1049.2		
1:1	$2\nu_2$	1063.6 , 1066		
1:1	ν_2		1595.0, 1598.0	
H_2O	ν_2 (nrm ^b)		1595.6	
1:1	$2\nu_1$	1707.2 , 1728.1		
OCS	$2\nu_1$	1714.8		
OCS	$\nu_1+2\nu_2$	1896.3		
1:1	$\nu_1+2\nu_2$	1903, 1907.7, 1911.2		
1:1	ν_3	2047.3 , 2048.7, 2050.7, 2054.1, 2055.2		
OCS	ν_3	2060.5, 2061.8, 2062.2		
1:1	ν_3+115	2172.3		
1:1	$\nu_1+\nu_3$	2901.7 , 2904.9, 2907.3		
OCS	$\nu_1+\nu_3$	2920.1		
OCS	$2\nu_2+\nu_3$	3097.9		
1:1	$2\nu_2+\nu_3$	3101.2		
1:1	$2\nu_2$		3153.0, 3159.6	
1:1	ν_1		3656.5, 3658.8	
H_2O	ν_1 (nrm)		3665.4	
1:1	ν_3		3749.8, 3753.3	
H_2O	ν_3 (nrm)		3761.0	
1:1	ν_3+115		3862	
1:1	$2\nu_3$	4071.7 , 4074.5, 4078.2, 4087.2		
OCS	$2\nu_3$	4098		
1:1	$\nu_1+\nu_2$		5239.4	
1:1	$\nu_2+\nu_3$		5328.5	

^a ν_1 : frequencies of the intermolecular modes.

^bnrm: nonrotating monomer of H_2O (see text).

Similar groups of bands are observed near the natural isotopic O^{13}CS ν_3 (2009.2 cm^{-1}) and ^{18}OCS ν_3 (2026.1 cm^{-1}) shown in Fig. S1 of the [supplementary material](#). For each group of bands, the most intense bands are observed at 1994.8 and 2002.2 cm^{-1} , and at 2011.4 and 2019.8 cm^{-1} , for the ^{13}C and ^{18}O isotopes, respectively. The evolution of all these bands is therefore linear with the concentration of OCS when normalized on water monomer signatures. Therefore, they are assigned to the 1:1 complex. When the OCS concentration exceeds H_2O concentration by nearly 100–500 times, we observe at 2040.0 and at 2064.3 cm^{-1} (the most intense) new bands attributed to a 2:1 complex. The natural ($\text{O}^{13}\text{CS}-\text{OCS}$): H_2O isotopic counterpart of the 2064.3 cm^{-1} band is observed at 1999.5 cm^{-1} . Also, a triplet of bands around 2043 cm^{-1} , with a main band at 2042.4 cm^{-1} , is observed at large water concentration with their intensities following those of the water dimer. Hence they are the signature of a 1:2 complex, and isotopic counterparts are observed for $\text{O}^{13}\text{CS}-(\text{H}_2\text{O})_2$ at 1989.9 cm^{-1} . For the 1:2 and 2:1 complexes, annealing effects confirm these attributions because the bands grow significantly and follow those of water and OCS dimer, respectively. All

TABLE II. Observed frequencies (cm^{-1}) and assignments for OCS-(H_2O)₂ and (H_2O)₂ complexes isolated in solid neon.

n:m	Assignment	OCS	H ₂ O	ν_i^a
1:2				201
1:2	ν_2		1597.2 PA, 1615.6 PD	
(H ₂ O) ₂	ν_2		1599.2 PA, 1616.5 PD	
1:2	$2\nu_1$	1699		
1:2	ν_2+201		1802	
1:2	ν_3	2042.4		
1:2	$2\nu_2$		3165.8 PA, 3202.0 PD	
(H ₂ O) ₂	$2\nu_2$		3163.0 PA, 3193.7 PD	
1:2	$\nu_1 \text{OH}_{b1}$		3569.5	
(H ₂ O) ₂	ν_1		3590.5 PD, 3660.6 PA	
1:2	$\nu_1 \text{OH}_{b2}$		3642.1	
1:2	$\nu_3 \text{OH}_f$		3740.6	
(H ₂ O) ₂	ν_3		3733.7 PD, 3763.5 PA	
1:2	$2\nu_3$	4061.9		
1:2	$\text{OH}_{b1}+\nu_2$		5163.8	
1:2	$\text{OH}_{b2}+\nu_2$		5224.3	
1:2	$\nu_2+\nu_3$		5320.0	
1:2	$2\nu_2+\nu_3$		6869.4	
1:2	$2\nu_3\text{OH}_{b2}$		7151.3	

^a ν_i : frequencies of the intermolecular modes.

the bands observed for these complexes are summarized in Tables I–III.

Since the C–S stretching vibration (ν_1) intensity is almost two orders of magnitude weaker in comparison with the CO vibration, OCS concentration must be elevated (7.5/1000 or 15/1000) to be observable [Fig. 2(a)]. The signature of ν_1 is at 860.9 cm^{-1} for OC³²S and at 849.6 cm^{-1} for OC³⁴S. When water is codeposited with OCS, we attribute the bands at 857.2 and 867.6 cm^{-1} to the 1:1 complex because of their linear evolution with OCS and water concentration [Fig. 2(b)]. As in the OCS ν_3 region, we also observe 2:1 absorption at 855.2

TABLE III. Observed frequencies (cm^{-1}) and assignments for (OCS)₂-H₂O and (OCS)₂ complexes isolated in solid neon. Most intense bands are in bold.

n:m	Assignment	OCS	H ₂ O	ν_i^a
2:1				105
2:1				180
(OCS) ₂	ν_2	521.3		
2:1	ν_1	855.2 , 866.2		
(OCS) ₂	ν_1	858.3		
2:1	ν_2		1591.8, 1593.4	
2:1	$2\nu_1$	1703.4, 1725.8		
2:1	ν_3	2040.0, 2064.3		
(OCS) ₂	ν_3	2067.6		
(OCS) ₂	$\nu_1+\nu_3$	2924.9		
2:1	$\nu_1+\nu_3$	2922.9		
2:1	$2\nu_2$		3146.6, 3149.1	
2:1	$\nu_1 \text{OH}_b$		3648.0	
2:1	$\nu_3 \text{OH}_f$		3741.0	
2:1	ν_3+180		3923	
2:1	$\nu_1+\nu_2$		5230.9	
2:1	$\nu_2+\nu_3$		5324.9	

^a ν_i : frequencies of the intermolecular modes.

(the most intense) and 866.2 cm^{-1} confirmed by annealing and concentration effects [Figs. 2(c) and 2(c')].

Near the OCS bending mode (ν_2) at 521.7 cm^{-1} , when H₂O is added, a new blue shifted signature appears at 529.2 cm^{-1} with a shoulder at 530.5 cm^{-1} that we attribute to the 1:1 complex (Fig. 3). Peaks at 503.6 and 507.0 cm^{-1} are assigned to O¹²CS–O¹³CS and O¹³CS, respectively. No band is detectable for the 2:1 and 1:2 complexes in this region.

B. H₂O spectral regions

Figure 4 shows the region of the water bending mode ν_2 . When adding OCS, two bands appear at 1595.0 and 1598.0 cm^{-1} on both sides of the ν_2 of the nonrotating monomer (nrm) H₂O³⁰ at 1595.6 cm^{-1} . They are attributed to the 1:1 complex due to their evolution with concentrations. Other signatures at 1593.4 and 1591.8 cm^{-1} are observed when the OCS concentration is high and follow the intensity of the OCS dimer, so they are assigned to the 2:1 complex. The same argument can be used for the observed bands at 1597.2 and 1615.6 cm^{-1} which follow the evolution of the H₂O dimer, so we attribute them to the 1:2 complex. The annealing effect at 12 K confirms the stoichiometry of the 2:1 and 1:2 complexes because it permits diffusion of the molecules in the samples and enhances the intensity of the bands of the complexes with higher stoichiometry.

In the ν_1 symmetric O–H stretching region (Fig. 5), a band at 3658.8 cm^{-1} and a small one at 3656.5 cm^{-1} appear when OCS is deposited with water, and they are attributed to the 1:1 complex. At higher water concentration, two bands grow at 3569.5 and 3641.3 cm^{-1} , near the ν_1 proton donor (PD) and proton acceptor (PA) molecules of the water dimer at 3590.5 and 3660.6 cm^{-1} , respectively, and these bands are attributed to the two bonded OH stretching (OH_b) of the 1:2 complex. At higher OCS concentration, a band attributed to the 2:1 complex appears at 3648.0 cm^{-1} . Other bands at 3521, 3546, and 3543 cm^{-1} appear when the OCS concentration greatly exceeds H₂O concentration, nearly 100–500 times higher, and correspond to larger complexes.

The region of the ν_3 asymmetric O–H stretching mode is characterized by the absorptions of the PD and PA molecules of the water dimer at 3733.7 and 3763.5 cm^{-1} , and the P(1) transition of the monomer at 3735.8 cm^{-1} (Fig. 6). But two weak bands grow with OCS concentration at 3753.3 and 3749.8 cm^{-1} and are therefore the signature of the 1:1 complex. When the concentration of OCS is very high, a band at 3741.0 cm^{-1} appears and is associated to the 2:1 complex. We also observe a band at 3740.6 cm^{-1} at higher water concentration attributed to the free OH stretching of the 1:2 complex.

C. Intermolecular vibrations

We investigated the far infrared to observe the intermolecular modes. In addition to the two water dimer bands and to the trimer band at 122, 170, and 150 cm^{-1} , respectively, four new bands appear at 105, 115, 180, and 201 cm^{-1} (Fig. 7). Due to their concentration evolution, the band at 115 cm^{-1} is the signature of the 1:1 complex, those at 105 and 180 cm^{-1} are the signatures of the 2:1 complex, and that at 201 cm^{-1} is

the characteristic of the 1:2 complex. These assignments for complexes with $n, m > 1$ are confirmed by the increase of their signature intensity under annealing at 12 K [Fig. 7(b')].

D. Multiquanta transitions

Near the $2\nu_2$ first overtone of the OCS bending mode at 1049.2 cm^{-1} , we observe two bands at 1066.7 and 1063.6 cm^{-1} spaced by twice the difference between the two ν_2 bands of the 1:1 complex, so we associate them to the $2\nu_2$ of the 1:1 complex. The $2\nu_1$ bands are observed at 1728.1 and 1707.2 cm^{-1} for 1:1, at 1699.0 cm^{-1} for 1:2, and at 1703.4 cm^{-1} for 2:1 (Fig. S2 of the [supplementary material](#)) (Tables I–III). Near the $\nu_1+\nu_3$ combination bands of OCS at 2920 cm^{-1} , we observe a similar triplet pattern as for the ν_3 of 1:1 corresponding to the $\nu_1+\nu_3$ transition at 2901.7 , 2904.9 , and 2907.3 cm^{-1} . Due to concentration effects, another band can be attributed to the 2:1 complex at 2922.9 cm^{-1} . In the OCS $2\nu_3$ region near 4101 cm^{-1} , we observe the signatures of 1:1 at 4071.7 , 4074.5 , 4078.2 , and 4087.2 cm^{-1} and of 1:2 4061.9 cm^{-1} .

In the $2\nu_2$ water region, the 1:1 bands are observed at 3153.0 and 3159.6 cm^{-1} and the 2:1 bands at 3146.6 and 3149.1 cm^{-1} . Signatures of the 1:2 complex are at 3165.8 and 3202.0 cm^{-1} , near the $2\nu_2$ overtone of the H_2O dimer bending mode. In the near infrared by comparison with data on the water monomer, we can attribute bands at 5239.4 and 5230.9 cm^{-1} to the $\nu_1+\nu_2$ combination of the 1:1 and 2:1 complexes, respectively. Similarly, bands at 5328.5 , 5324.9 , and 5320.0 cm^{-1} correspond to the $\nu_2+\nu_3$ combination for the 1:1, 2:1, and 1:2 complexes respectively. Finally, specifically for the 1:2 complex, we observe other combinations and overtones up to 7150 cm^{-1} (Table II), and the assignment is done by comparison with data on the water dimer in solid neon.²⁴

We also observe combinations of intra+intermolecular modes that confirm the attribution of the intermolecular modes in the far infrared. Indeed, at 2172.3 cm^{-1} we observe a 1:1 band which is the combination of the OCS ν_3 with the intermolecular vibration at 115 cm^{-1} . Two other intra+inter combination bands are observed at 3862 and 3923 cm^{-1} : the first one for 1:1, corresponding to $\text{H}_2\text{O } \nu_3 + 115\text{ cm}^{-1}$, and the last one for 2:1, corresponding to $\text{H}_2\text{O } \nu_3 + 180\text{ cm}^{-1}$. For the 1:2 complex, a band at 1802 cm^{-1} is the combination of the $\text{H}_2\text{O } \nu_2$ mode, at 1615.6 (PD) or 1597.2 (PA) cm^{-1} , with the intermolecular band at 201 cm^{-1} , that give sums of $1615.6 + 201 = 1816.6$ or $1597.2 + 201 = 1798.2\text{ cm}^{-1}$. It is impossible to determine if it is the combination with the PA or the PD of the water dimer subunit.

IV. THEORETICAL RESULTS

A. OCS– H_2O complex

Several theoretical studies have been carried out on the 1:1 complex.^{3–10} However, a disagreement exists on the different possible isomers (structures F1, F2, and F3 of Fig. 8). Wójcik *et al.* only found the F2 structure (MP2/6-31++g**).³ Tatamitani and Ogata¹⁰ only found the F1 structure (MP2 with several double zeta Pople basis set), as well as Garden *et al.* [CCSD(T)/aug-cc-pv(T+d)Z].⁵ Hartt *et al.* found the three structures [MP2/AVTZ and CCSD(T)/AVTZ single point calculations at MP2/AVDZ optimized geometries].⁴

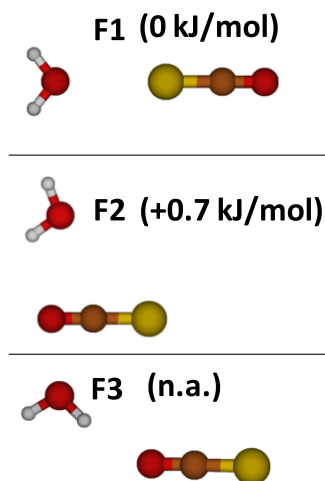


FIG. 8. Geometries of the F1, F2, and F3 isomers for the 1:1 OCS– H_2O complex. Relative energies corrected from ZPE computed at CCSD(T)-F12a/AVTZ level of theory. (n.a.) Relative energy not available at CCSD(T)-F12a (see text).

Ghosh *et al.* found the F1 and F2 structures [CCSD(T)/cc-pvTZ single point at MP2/6-311++G(2d,2p) geometries].⁶

In agreement with the work of Hartt *et al.*⁴ our MP2/AVTZ calculations lead to the three structures with D_e values of -8.6 , -8.9 , and -8.7 kJ/mol and D_0 values of -6.6 , -5.5 , and -5.1 kJ/mol for F1, F2, and F3, respectively. However, the F3 structure seems to be an artefact of MP2 because all optimisations of this geometry at the higher level of theory CCSD(T)-F12a/AVTZ lead to the nearest stable structure F2. At this level of theory, only F1 and F2 are minima on the potential energy hypersurface with D_e values of -8.2 and -8.7 kJ/mol and D_0 values of -6.2 and -5.5 kJ/mol for F1 and F2, respectively. The F1 isomer is computed to be the most stable and corresponds to the one observed in the microwave study¹⁰ with a C_{2v} symmetry, the sulphur atom interacting with the water oxygen atom. The F2 isomer is slightly less stable ($+0.7\text{ kJ/mol}$) and has a weak hydrogen bond between the oxygen of OCS and a hydrogen atom of water. Cartesian coordinates, energies, and vibrations of the F1 and F2 isomers are given in the [supplementary material](#) as well as those of monomers for both MP2/AVTZ and CCSD(T)F12a/AVTZ level of theory.

For larger complexes, our computing resources do not allow us to optimize and to compute frequencies at CCSD(T)-F12a/AVTZ level of theory. Therefore, ground state binding energies were computed from single point CCSD(T)-F12a/AVTZ calculations at MP2/AVTZ optimized geometries, corrected from MP2/AVTZ zero point energy for D_0 . In the case of the 1:1 complex, this procedure leads to an error less than 0.2 kJ/mol with D_e^* values of -8.2 and -8.8 kJ/mol and D_0^* values of -6.1 and -5.3 kJ/mol for F1 and F2, respectively.

B. OCS–(H_2O)₂ and (OCS)₂– H_2O complexes

According to Hartt *et al.*,⁴ we found two isomers for the 1:2 complex formed by an OCS molecule interacting with a water dimer. We only report the most stable complex in Fig. 9 which has a D_0^* value of -25.8 kJ/mol , as the other one is 4 kJ/mol less stable. The 1:2 complex is formed by an OCS

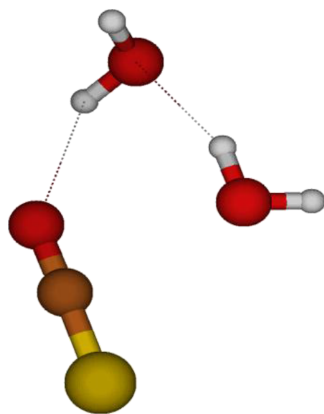


FIG. 9. MP2/AVTZ geometry of the most stable isomer of the 1:2 complex.

molecule linked to a slightly distorted water dimer. Cartesian coordinates, energies, and vibrations of the two structures of the 1:2 complex are given in the [supplementary material](#) as well as those of the water dimer at the same level of calculation.

Before studying the 2:1 complex, it is necessary to first investigate the OCS dimer. Four geometries (S1, S2, S3, and S4) are found to be probable (Fig. 10), and the calculated D_0^* are equal to -6.4 , -5.7 , -5.5 , -5.2 kJ/mol respectively. These values are very similar to the results of Refs. 12 and 13. Cartesian coordinates, energies, and vibrations of the four structures are given in the [supplementary material](#).

For the 2:1 complex, four stable forms, A1, A2, A3, and A4 (Fig. 11), have been found with D_0^* equal to -17.0 , -16.6 , -16.5 , and -15.0 kJ/mol, respectively. A1 has a C_s symmetry and is formed by a non-polar OCS dimer S1 with a hydrogen bonded to an oxygen of OCS. A2, A3, and A4 are formed by a nonpolar (S1), a polar (S2), and a nonpolar (S3) tilted OCS dimer, respectively, where H_2O is intercalated between the OCS molecules. Cartesian coordinates, energies, and vibrations of the four isomers are reported in the [supplementary material](#).

As A4 is the less stable isomer, the difference of stability compared with the others forms is between $+1.5$ and $+2$ kJ/mol,

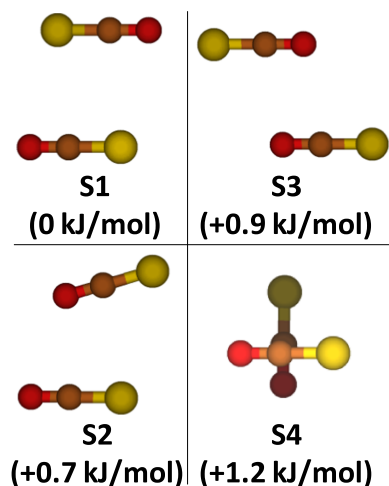


FIG. 10. Calculated geometries of the 2:0 complex. Relative energies computed at CCSD(T)-F12a/AVTZ from MP2/AVTZ structures and corrected from MP2/AVTZ ZPE.

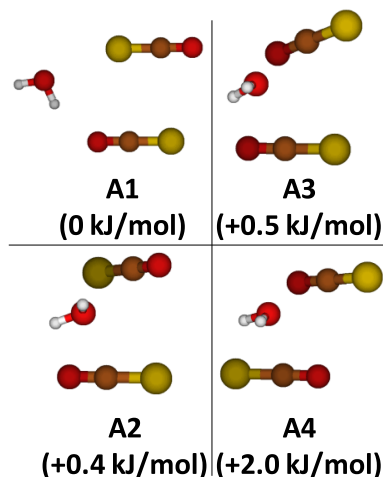


FIG. 11. Calculated geometries of the 2:1 complex. Relative energies computed at CCSD(T)-F12a/AVTZ from MP2/AVTZ structures and corrected from MP2/AVTZ ZPE.

which is rather high so it will be dismissed from the vibrational assignments and discussion.

V. VIBRATIONAL ASSIGNMENTS AND DISCUSSION

For such weak van der Waals complexes, following the effect of complexation by using the vibrational shift between the monomer and complexes ($\Delta\nu = \nu_{\text{mono}} - \nu_{\text{complex}}$) is a good spectroscopic diagnosis to match the observed bands with modes of the different complexes. The comparison between the theoretical and experimental $\Delta\nu$ values is helpful to attribute the experimental observations.

A. OCS- H_2O complex

The fundamental bands of the 1:1 complex are easily assigned without ambiguity due to concentration effects. Some of them are multiple and they cannot be only different trapping sites since the frequency shifts between the bands are too large.³¹ The experimental and calculated vibrations for

TABLE IV. Comparison of frequencies (cm^{-1}) and shifts ($\Delta\nu = \nu_{\text{mono}} - \nu_{\text{complex}}$) for F1 and F2 1:1 complexes between observed and calculated (MP2/AVTZ) data.

	H ₂ O modes				OCS modes			
	Calc.		Exp.		Calc.		Exp.	
	F1	F2	F1	F2	F1	F2	F1	F2
ν_3	3941 (82) ^a	3939 (80)	3753.3 (10) ^b	3749.8 (3.5)	2073 (680)	2082 (650)	2047.3 (1000) ^c	2055.2 (170)
$\Delta\nu$	+7	+9	+7.7	+11.2	+11	+2	+14.4	+7.0
ν_1	3816 (10)	3812 (3)	3658.8 (6.2)	3656.5 (1.3)	883 (3)	894 (4)	857.2 (4.3) ^c	867.6 (0.5) ^c
$\Delta\nu$	+6	+10	+6.6	+8.9	+5	-6	+4.0	-7.0
ν_2	1630 (72)	1622 (150)	1598.0 (40)	1595.0 (33)	532 (1)	523 (1)	529.2 (9.8) ^c	529.2 (9.8) ^c
$\Delta\nu$	-2	+6	-2.4	+0.6	-9	0	-7.5	-7.5

^aCalculated intensities in km/mol in parentheses.

^bExperimental intensities relative to OCS ν_3 ($I_{\nu_3} = 1000$) in parentheses.

^cSum of matrix sites intensities.

the two 1:1 isomers as well as the intensities and the shifts are given in Table IV, and calculated harmonic frequencies values at the MP2 level for the H₂O and OCS monomers are given in the [supplementary material](#) as well as the intermolecular modes of the 1:1 complexes. Some calculated shifts between the two isomers are significantly different and will be helpful to attribute the experimental observations to a specific isomer.

As theoretical calculations have found two stable close energy isomers, we compare the experimental and theoretical vibrational shifts to interpret the observed signatures by the presence of these two isomers. The calculated frequencies are comparable with those given by the literature.⁴⁻⁸ The assignments of the different vibrations to F1 and F2 isomers are also summarized in Table IV.

In the water ν_3 region, the bands attributed to 1:1 at 3753.3 and 3749.8 cm⁻¹ are attributed to F1 and F2, respectively, since the experimental shifts are +7.7 and +11.2 cm⁻¹ and the calculated ones +7 and +9 cm⁻¹ for F1 and F2. A similar attribution can be done for the two bands of the ν_1 and ν_2 modes, observed at 3658.8 and 3656.5 cm⁻¹ and at 1598.0 and 1595.0 cm⁻¹, respectively (Table IV).

The ν_3 vibration of the OCS submolecule is composed of two groups of bands red shifted with respect to OCS monomer absorption. The main band of the first one has a $\Delta\nu$ of +14.4 and the calculated one is +11 cm⁻¹ for F1. The main band of the second one has a $\Delta\nu$ of +7.0 cm⁻¹ and this value is higher than those calculated at +2 cm⁻¹ for the F2 isomer. Since the calculated and observed vibrational shifts between the two isomers F1 and F2 is the same, 9 and 8 cm⁻¹, respectively, we attribute the more red shifted band to the F1 isomer, and the other to the F2 one.

For the two bands of the ν_1 mode at 867.6 and 857.2 cm⁻¹, the assignment to F2 and F1, respectively, is easy since these bands are blue and red shifted, respectively, and this is the main difference between the two isomers. For ν_2 , the weaker fundamental mode, we conclude that we only observe the F1 isomer because the experimental shift is very near to the calculated one. We do not see the F2 isomer signature which is in agreement with the calculation which predicts this band very near the monomer one. Finally, we associate the observed intermolecular band at 115 cm⁻¹ to the calculated one at 109 cm⁻¹ (intermolecular in plane H₂O bending, see the [supplementary material](#)) of F1, most populated form, because it is the calculated most intense mode in the observed region.

By comparison between experimental and theoretical fundamental modes, we have identified two isomers in solid neon, not surprising because they are calculated close in energy. The calculated intensities of the modes for the isomers are very near, and as the experimental bands intensities of the F1 isomer are more intense than those of F2, it could indicate a higher F1 concentration formed in the matrix which is in agreement with the fact that F2 is computed to be 0.7 kJ/mol less stable than F1.

For the multiquanta transitions, we clearly observe two combinations with the only observed intermolecular mode, at 115 cm⁻¹, with the water and OCS ν_3 modes (Table I). These combinations show a small anharmonicity coefficient X_{ij} , in agreement with other water-molecule complexes.^{2,24,32}

For the combination mode at 2172.3 cm⁻¹, we can deduce an anharmonicity coefficient of +8.6 cm⁻¹, near the value for the similar combination in the CO₂-H₂O complex.²

For H₂O modes, the X_{12} , X_{22} , and X_{23} values (-17.4, -18.2, and -22.8 cm⁻¹, respectively) are very similar to those of the H₂O monomer (-17.0, -19.0, and -19.4 cm⁻¹, respectively), and the couplings between the water modes are not perturbed by the presence of OCS. For the OCS modes, we observe the $2\nu_1$, $2\nu_2$, and $2\nu_3$ overtones and the $\nu_1+2\nu_2$, $\nu_1+\nu_3$, and $2\nu_2+\nu_3$ combinations (Table I). The deduced anharmonicity coefficients X_{11} , X_{12} , X_{13} , X_{23} , X_{22} , and X_{33} (-3.5, -6.9, -3.0, -6.8, +2.9, and -13.6 cm⁻¹, respectively) are the same in comparison with those of the OCS monomer (-3.5, -6.9, -3.0, -6.8, +2.9, and -13.6 cm⁻¹, respectively). Also, the observation of the $\nu_1+\nu_3$ is important because the observed value, 2901.7 cm⁻¹, is the combination of the bands at 2047.3 and 857.2 cm⁻¹. It fully confirms that these bands belong to the same isomer F1, in agreement with the calculations.

We should mention that frequency shifts obtained at CCSD(T)-F12a/AVTZ level of theory (not reported in Table IV) are very similar to those obtained with MP2/AVTZ and lead to the same attribution of observed frequencies. This confirms that MP2/AVTZ is sufficient to assign the bands observed for the 1:2 and 2:1 complexes presented in the following paragraphs.

B. OCS-(H₂O)₂ complex

The water vibrations of 1:2 are compared with those of the water dimer (Table V). The effect of OCS on the stretching modes of the water dimer is significant (around 20 cm⁻¹), while the bending is slightly perturbed. The most stable calculated geometry of the 1:2 complex (Fig. 9) is clearly a water dimer where the oxygen of the OCS molecule is linked to a hydrogen of the water dimer. The calculated shifts agree quite well with the experimental ones except for the ν_3 OCS mode without explanation. The observed intermolecular frequency at 201 cm⁻¹ can be identified as the most intense calculated one at 267 cm⁻¹ and can be unambiguously assigned to the intermolecular in plane H₂O bending with the help of *ab initio* calculations (see the [supplementary material](#)).

At 1802 cm⁻¹, we observe a combination of one water ν_2 mode (PA or PD) and the intermolecular mode at 201 cm⁻¹, and we can deduce anharmonicity coefficients equal to -14.6 cm⁻¹ for PD mode or +3.8 cm⁻¹ for PA mode but we cannot conclude which one of these two modes is observed.

TABLE V. Experimental and calculated (MP2/AVTZ) frequencies shifts (cm⁻¹) between the 1:2 complex and the H₂O dimer, and the OCS monomer.

	$\Delta\nu = \nu(\text{H}_2\text{O})_2 - \nu(1:2)$		$\Delta\nu = \nu(\text{OCS}) - \nu(1:2)$	
	Exp.	Calc.	Exp.	Calc.
$\Delta\nu_3$	+22.9 PA +19 PA	+16 PA +24 PA	+19.8	0
$\Delta\nu_1$	+21 PD +2 PA	+32 PD -1 PA		
$\Delta\nu_2$	+0.9 PD	-3 PD		

TABLE VI. Experimental and calculated (MP2/AVTZ) frequencies shifts (cm^{-1}) between the 2:1 complex and the OCS monomer, dimer, and the H_2O monomer.

	$\Delta v = \nu(\text{H}_2\text{O}) - \nu(2:1)$				$\Delta v = \nu(\text{OCS}) - \nu(2:1)$				$\Delta v = \nu(\text{OCS})_2 - \nu(2:1)$				
	Exp.	A1 ^a	A2	A3	Exp.	A1	A2	A3	Exp.	A1 S1 ^b	A1 S2	A1 S3	A1 S4
Δv_3	+20.0	+20	+13	+17	-2.1 ^c	-4	-10	-6	+3.3	+5	+2	-6	-4
					+21.2	+20	+8	+9		+7	+12	+18	+17
Δv_1	+17.4	+20	+14	+17	-5.3	-8	-4	-5	-8.0	-9	-7	-5	-7
					+5.7	+4	+1	-3	+3.1	+3	+2	+6	+5
Δv_2	+2.2	-2	+5	+1									

^aA1, A2, and A3 are the three calculated isomers for the 2:1 complex.

^bS1, S2, S3, and S4 are the four calculated isomers for the OCS dimer (Fig. 10).

^cFor each OCS vibration, the first line corresponds to the out-of-phase vibration and the second line to the in-phase vibration (see text).

For OCS modes, the 1:2 complex has the same X_{33} coefficient (-11.5 cm^{-1}) compared to the 1:1 complex. For H_2O modes, the coefficients X_{11} , X_{12} , X_{22} , and X_{23} $\{-65.5, [-15(\text{PA}), -21.3(\text{PD})], [-12.1(\text{PA}), -14.6(\text{PD})], -17.8 \text{ cm}^{-1}\}$ are comparable with those of the water dimer $\{-57.3, [-17(\text{PA}), -15.8(\text{PD})], [-17.7(\text{PA}), -19.7(\text{PD})], -20.2 \text{ cm}^{-1}\}$.

C. $(\text{OCS})_2\text{-H}_2\text{O}$ complex

Our work is the first report on experimental and calculated data on the 2:1 complex. In Table VI we compare the experimental shifts with the theoretical ones for the three calculated 2:1 isomers [A1, A2, and A3 (Fig. 11)]. The comparison between the water vibrations with those in the H_2O monomer shows that the ν_2 mode is weakly perturbed ($\Delta v = +2.2 \text{ cm}^{-1}$) in contrast to the stretching modes ν_3 and ν_1 ($\Delta v = +20$ and $+17.4 \text{ cm}^{-1}$, respectively). The observed OCS ν_3 and ν_1 bands are minimally red shifted due to the OCS monomer or dimer, so the OCS dimer is weakly perturbed by the presence of one water molecule. If we focus on the shifts between experimental and calculated of $\Delta v = \nu(\text{H}_2\text{O}) - \nu(2:1)$, A2 isomer can be discarded. The comparison with the OCS monomer is more complicated since the 2:1 complex contains two OCS molecules, and there are two intramolecular vibrational fundamentals associated with the ν_3 and ν_1 monomer stretch fundamentals (the in-phase and the out-of-phase vibration of the two monomers). For this reason, there are two lines in Table VI for the OCS vibrations. The best match with the experimental shifts is clearly obtained for the A1 isomer. Finally, the comparison with the four calculated OCS dimers shows that the calculated shifts for the S3 and S4 isomers are too different from the experimental ones. The agreement of the experimental shifts with those from the OCS dimers S1 and S2 are very similar. In our study we cannot conclude which OCS dimer is observed in the Ne matrix. The McKellar group has observed in gas phase the OCS dimers S1¹⁵ and S2^{16,17} in the ν_3 region at 2069.3 and 2072.0 cm^{-1} , respectively, and our Ne values is at 2067.6 cm^{-1} .

We observe two signatures of the 2:1 complex in the intermolecular region at 105 and 180 cm^{-1} . When we compare them with the intense calculated modes for the A1 isomer, these bands can be assigned to the modes at 97 cm^{-1} (the intermolecular out of plane H_2O bending) and 214 cm^{-1} (the intermolecular in plane H_2O bending, see the [supplementary](#)

[material](#)), respectively. The attribution of the band at 180 cm^{-1} is confirmed by the observation at 3923 cm^{-1} of the combination between this intermolecular mode and the ν_3 band at 3741 cm^{-1} that gives an anharmonicity of 2 cm^{-1} . This weak value is in agreement with intra+inter combination in a water dimer, trimer, or hydrated complex.^{23,24,32}

As well, we can compare the deduced anharmonicity coefficients X_{11} and X_{13} equal to -3.5 and $+2.4 \text{ cm}^{-1}$, respectively. For the H_2O modes, the X_{22} value, -18.8 cm^{-1} , is very similar to that of the H_2O monomer and 1:1 complex (-19.0 and -18.2 cm^{-1} , respectively) but the X_{12} and the X_{23} values (-10.0 and -9.5 cm^{-1} , respectively) are nearly half the value of those in the H_2O monomer (-17 , -19.4 cm^{-1}) and 1:1 complex (-14.0 , -22.8 cm^{-1}). Note that the large decrease of these coefficients is correlated to the decoupling of the two OH oscillators, as suggested in the literature.³³

VI. CONCLUSION

For the first time, a neon matrix isolation study of the $(\text{OCS})_n(\text{H}_2\text{O})_m$ complexes has been carried out from the far to the near infrared spectral range. On the basis of concentration and annealing effects, and with the support of theoretical calculation, the existence of two isomers has been highlighted for the 1:1 complex with the observation for each isomer of the three water modes perturbed by OCS, and for two OCS modes perturbed by water. The 1:2 and 2:1 complexes have been identified and compared with the 2:0 and 0:2 dimers. Careful examination of the far infrared region allows the assignment of 1:1, 2:1, and 1:2 intermolecular modes, confirmed by the observation of intra+intermolecular combinations. Anharmonicity coefficients X_{ij} have been deduced, thanks to the observation of overtones and combination bands. So the isolation neon matrix technique allows to implement the study of very weak binding complexes ($E < 5.9 \text{ kJ/mol}$) potentially useful for gas phase experiment and to highlight the existence of different isomers for the 1:1 complex. Some anharmonic experimental data will be useful for new theoretical investigations at the anharmonic level.

SUPPLEMENTARY MATERIAL

See [supplementary material](#) for Cartesian coordinates, energies, harmonic frequencies, and intensities computed for

OCS and water monomers, and the most stable isomers of the 1:1, 2:0, 0:2, 1:2, and 2:1 complexes. Two figures in this show the OCS stretching ν_3 region of the $\text{O}^{13}\text{CS}-\text{H}_2\text{O}$ and $^{18}\text{OCS}-\text{H}_2\text{O}$ complexes and the $2\nu_1$ overtone region of the OCS.

- ¹V. Vaida, *J. Chem. Phys.* **135**, 020901 (2011).
- ²P. Soulard and B. Tremblay, *J. Chem. Phys.* **143**, 224311 (2015).
- ³M. J. Wójcik, M. Boczar, and T. A. Ford, *Chem. Phys. Lett.* **348**, 126 (2001).
- ⁴G. M. Hartt, G. C. Shields, and K. N. Krischner, *J. Phys. Chem. A* **112**, 4490 (2008).
- ⁵A. L. Garden, J. R. Lane, and H. G. Kjaergaard, *J. Chem. Phys.* **125**, 144317 (2006).
- ⁶D. Ghosh, B. Mondal, S. Bagchi, and A. K. Das, *Mol. Phys.* **108**, 3353 (2010).
- ⁷P. Ramasami and T. A. Ford, *Mol. Phys.* **112**, 683 (2014).
- ⁸P. Ramasami and T. A. Ford, *J. Mol. Struct.* **1072**, 28 (2014).
- ⁹S. Mondal, A. U. Teja, and P. C. Singh, *J. Phys. Chem. A* **119**, 3644 (2015).
- ¹⁰Y. Tatamitani and T. Ogata, *J. Chem. Phys.* **121**, 9885 (2004).
- ¹¹X. H. Li, S. J. Ren, X. G. Wei, Y. Zeng, G. W. Gao, Y. Ren, J. Zhu, K. C. Lau, and W. K. Li, *J. Phys. Chem. A* **118**, 3503 (2014).
- ¹²J. Brown, X. G. Wang, R. Dawes, and T. Carrington, Jr., *J. Chem. Phys.* **136**, 134306 (2012).
- ¹³N. Sahu, G. Singh, and S. R. Gadre, *J. Phys. Chem. A* **117**, 10964 (2013).
- ¹⁴R. G. A. Bone, *Chem. Phys. Lett.* **206**, 260 (1993).
- ¹⁵M. Afshari, Z. Abusara, N. Dehghani, N. Moazzen-Ahmadi, and A. R. W. McKellar, *Chem. Phys. Lett.* **437**, 23 (2007).
- ¹⁶M. Afshari, N. Dehghani, Z. Abusara, N. Moazzen-Ahmadi, and A. R. W. McKellar, *Chem. Phys. Lett.* **442**, 212 (2007).
- ¹⁷M. Afshari, M. Dehghani, Z. Abusara, N. Moazzen-Ahmadi, and A. R. W. McKellar, *J. Chem. Phys.* **126**, 071102 (2007).
- ¹⁸T. H. Dunning, *J. Chem. Phys.* **90**, 1007 (1989).
- ¹⁹R. A. Kendall, T. H. Dunning, and R. J. Harrison, "Electron-affinities of the 1st-row atoms revisited. Systematic basis-sets and wave-functions," *J. Chem. Phys.* **96**, 6796 (1992).
- ²⁰M. J. Frisch, G. W. Trucks, H. B. Schlegel *et al.*, GAUSSIAN 09, Revision D.01, Gaussian, Inc., Wallingford, CT, 2009.
- ²¹H. J. Werner, P. J. Knowles, G. Knizia, F. R. Manby, and M. Schutz, "Molpro: A general-purpose quantum chemistry program package," *Wiley Interdiscip. Rev.: Comput. Mol. Sci.* **2**, 242 (2012).
- ²²H. J. Werner, P. J. Knowles, G. Knizia, F. R. Manby *et al.*, MOLPRO, version 2012.1, a package of *ab initio* programs, 2012, see <http://www.molpro.net>.
- ²³Y. Bouteiller, B. Tremblay, and J. P. Perchard, *Chem. Phys.* **386**, 29 (2011).
- ²⁴B. Tremblay, B. Madebène, M. E. Alikhani, and J. P. Perchard, *Chem. Phys.* **378**, 27 (2010).
- ²⁵V. I. Lang and J. S. Winn, *J. Chem. Phys.* **94**, 5270 (1991).
- ²⁶F. D. Verderame and E. R. Nixon, *J. Chem. Phys.* **44**, 43 (1966).
- ²⁷M. Afshari, M. Dehghani, Z. Abusara, N. Moazzen-Ahmadi, and A. R. W. McKellar, *J. Chem. Phys.* **127**, 144310 (2007).
- ²⁸L. Evangelisti, C. Perez, N. A. Seifert, B. H. Pate, M. Dehghany, N. Moazzen-Ahmadi, and A. R. W. McKellar, *J. Chem. Phys.* **142**, 104309 (2015).
- ²⁹A. Fayt, R. Vandenhoute, and J. G. Lahaye, *J. Mol. Spectrosc.* **119**, 233 (1986).
- ³⁰A. Engdahl and B. Nelander, *J. Mol. Struct.* **193**, 101 (1989).
- ³¹M. E. Jacox, *Chem. Soc. Rev.* **31**, 108 (2002).
- ³²M. Cirtog, P. Asselin, P. Soulard, B. Tremblay, B. Madebène, M. E. Alikhani, R. Georges, A. Moudens, M. Goubet, T. R. Huet, O. Pirali, and P. Roy, *J. Phys. Chem. A* **115**, 2523 (2011).
- ³³A. Burneau and J. Corset, *J. Chem. Phys.* **69**, 171 (1972).